

Canopy stomatal uptake of NO_x, SO₂ and O₃ by mature urban plantations based on sap flow measurement

Yanting Hu, Ping Zhao*, Junfeng Niu, Zhenwei Sun, Liwei Zhu, Guangyan Ni

Key Laboratory of Vegetation Restoration and Management of Degraded Ecosystems, South China Botanical Garden, Chinese Academy of Sciences, China

Abstract

Canopy stomatal uptake of NO_x (NO, NO₂), SO₂ and O₃ by three mature urban plantations (of *Schima superba*, *Eucalyptus citriodora* and *Acacia auriculaeformis*) were studied using the sap flow-based approach under free atmospheric conditions. The annual mean concentration for NO, NO₂, SO₂ and O₃ were 18.17, 58.05, 12.76 and 42.36 µg·m⁻³, respectively. The atmospheric concentration exhibited a spring or winter maximum for NO, NO₂ and SO₂, whereas the concentration maxima for O₃ occurred in the autumn. Despite the daytime mean canopy stomatal conductance (G_c) being positively related with the photosynthetically active radiation (PAR) and negatively with the vapour pressure deficit (VPD), the maximal daytime mean G_c did not appear when the PAR was at its highest level or the VPD was at its lowest level because a positive correlation was noted between the daytime mean PAR and VPD ($P<0.001$) under field conditions. The G_c value was regulated by the cooperation of the PAR and VPD . When analysing the [respective](#) effect of the PAR or VPD on G_c separately, a positive logarithmical correlation was noted between the daytime mean G_c and PAR as the following equation: ($P<0.01$), and the daytime mean G_c was negatively logarithmically correlated with the VPD : ($P<0.001$). The daytime mean G_c declined with decreases in the soil water content (SWC) under similar meteorological condition. Differences in the seasonal pattern of the canopy stomatal

* Corresponding author. Tel.: +86 020 37252881 ; fax: +86 020 37252831.

E-mail address: zhaoping@scib.ac.cn (P. Zhao).

conductance and atmospheric concentrations led to a differentiated peak flux. The flux for NO, NO₂ and SO₂ exhibited a spring maximum, whereas the flux maxima for O₃ appeared in the autumn or summer. The annual accumulative stomatal flux for NO, NO₂, SO₂ and O₃ was 100.19±3.76, 510.68±24.78, 748.59±52.81 and 151.98±9.33 mg·m⁻²·a⁻¹, respectively. When we focus on the foliar uptake of trace gases, the effect of these gases on the vegetation in turn should be considered, particularly for regions with serious air pollution problems. These trace gases had not yet reached injury levels, except for NO₂. Flux-based measurements were better suited for evaluating the risk of O₃ damage to vegetation than the exposure-based method.

Keywords: sap flow, canopy stomatal conductance, environmental factors, stomatal uptake

1. Introduction

Tropospheric concentrations of trace chemicals (such as NO_x, SO₂ and O₃) in the atmosphere have increased significantly within the last century (Löw *et al.*, 2012; Richter *et al.*, 2005; Seinfeld and Pandis, 2012; Smith *et al.*, 2011). One important potential consequence of this change is alteration to the climate (Ramanathan *et al.*, 1985). Studies of the radiative forcing of these chemically reactive species showed that NO_x emissions have a global cooling effect because they indirectly remove CH₄ by increasing the abundance of OH radicals and produce aerosols that cool the atmosphere (Schulze *et al.*, 2010). Sulphur dioxide is a principal precursor of sulphate aerosols, which may affect climate directly by reflecting solar radiation into space and indirectly by changing the reflective properties of clouds and their lifetimes (Karl and Trenberth, 2003). Tropospheric ozone (O₃), an important greenhouse gas, is responsible for direct radiative forcing (0.35-0.37 W·m⁻²) (Ainsworth *et al.*, 2012). Apart from their influences on the climate, trace chemicals are also important

atmospheric constituents responsible for air pollution. Atmospheric nitrogen oxides contribute to photochemical smog, the formation of acid rain precursors and the destruction of the ozone in the stratosphere (Bowman, 1992). Additionally, SO₂ is the major gaseous precursor of acidic precipitation (Vahedpour and Zolfaghari, 2011). Because of the negative influences that these trace gases display on the environment, regions with a high contamination level must reduce these gas concentrations to an acceptable level by focusing on controlling the source of air pollutants and on the removal of existing pollutants (Yang *et al.*, 2008).

In recent years, foliar uptake of trace gases has attracted interest (Eichert and Fernández, 2012). Trace gases enter the leaves predominantly through the stomata, and moreover, the stomatal uptake is a direct addition to plant metabolism and could potentially more readily influence plant growth depending on the concentration and plant species (Eichert and Fernández, 2012; Sparks, 2009). In addition, a critical level for the stomatal uptake is noted, beyond which the leaf detoxification systems are unable to cope with the stress induced by gas molecules (Josipovic *et al.*, 2010; Karlsson *et al.*, 2004). Thus, quantifying the stomatal fluxes of these pollutant gases is important. During the last few decades, several micrometeorological methods for quantifying trace gas exchange between the terrestrial ecosystem and atmosphere have been developed including the eddy covariance technique, aerodynamic profile method and Bowen ratio-energy balance method (Grünhage *et al.*, 2000). However, separating the stomatal deposition component from the overall flux using these methods remained difficult (Sparks, 2009). Additionally, dry deposition models are used to analyse trace gas exchange between the phytosphere and atmosphere. Despite the fact that stomatal uptake can be modelled, modelling methods display a common difficulty of estimating the physiological functions of plants. Because plant species

chinaXiv:201707.00074v1

differ considerably in their response to environmental conditions and because the effects of important environmental factors such as soil moisture are difficult to model realistically, stomatal conductance estimates are frequently inaccurate (Pleim *et al.*, 1999). Within the frame of such studies, appropriate methods to estimate the long-term and continuous aboveground stomatal uptake of gases by vegetation under natural atmospheric conditions must be developed (Köstner *et al.*, 2008).

The above outlined mechanistic shortcomings can be overcome through the sap flow approach, as recently suggested and demonstrated by Wieser *et al.* (2003), Matyssek *et al.* (2004), Nunn *et al.* (2007), Köstner *et al.* (2008) and Wang *et al.* (2012). The sap flow-based methodology contributes a new quality of flux data, significantly improving our understanding of biospheric aspects of trace-gas fluxes into tall vegetation (Köstner *et al.*, 2008). Trace gas flux at the canopy scale can be obtained from the concentration gradient between the atmosphere and the intercellular space, and the canopy stomatal conductance for trace gases derived from the conductance for water vapour (because transpiration and trace gas flux are coupled through the activity of the stomata) (Wieser *et al.*, 2006). Additionally, the stand transpiration and the [synchronous](#) meteorological data provide the basis for the calculation of the canopy stomatal conductance for water vapour. The stand transpiration can be estimated through the sap flow measurements combined with stand characteristics.

Rapid economic development during the past two decades has already led to regional air pollution problems over the Pearl River Delta (PRD) in South China (Zheng *et al.*, 2009). Studies have reported that high levels of ozone have been observed in the PRD region over the past few decades (Liu *et al.*, 2008; Wang *et al.*, 2003; Zhang *et al.*, 2008), and the ozone background concentrations increased by an

average rate of 0.55 ppbv·yr⁻¹ during 1994-2007 (Wang *et al.*, 2009). NO_x emissions also exhibited increasing trends during 2000-2009 (Lu *et al.*, 2013). Although the regional monitoring network data indicate a reduction of atmospheric SO₂ concentration because of the decrease in the SO₂ emissions (Wang *et al.*, 2013), the SO₂ concentration in the PRD region is still substantially higher than those reported for large cities in Europe and North America (Wan *et al.*, 2011). Urban vegetation is generally considered to be effective in mitigating various air pollution problems (Jim and Chen, 2008; Setälä *et al.*, 2013; Yang *et al.*, 2008; Yin *et al.*, 2011). In the present study, we investigated stomatal uptake of NO_x, SO₂ and O₃ by mature urban plantations (*S. superba*, *E. citriodora* and *A. auriculaeformis*) using the sap flow-based approach in Guangzhou City which is located in the central region of PRD, China. The main objectives are the following: (1) to analyze seasonal and [annual patterns](#) of the NO_x, SO₂ and O₃ concentrations, the canopy stomatal conductance and the fluxes of these trace gases between the vegetation canopy and the atmosphere; (2) to elucidate the relationship between the canopy stomatal conductance and environmental factors and the conditions under which the daytime mean canopy stomatal conductance (G_C) reaches a maximum; (3) to quantify the annual accumulative stomatal uptake of trace gases; (4) to evaluate whether the current situation reached a certain contamination degree using the exposure-based approach (De Vries *et al.*, 2000; Tao and Feng 2000) and the flux-based approach (Simpson *et al.*, 2007).

2. Methods

2.1. Site description

This research was conducted in *S. superba*, *E. citriodora* and *A. auriculaeformis* plantations located in the South China Botanical Garden, Guangzhou, China

(113°22'E, 23°11'N) during 2013. This region is typically dominated by a subtropical monsoon climate and experiences an annual precipitation of 1696.5 mm and an annual average temperature of 21.9. The *S. superba*, *E. citriodora* and *A. auriculaeformis* plantations have been planted since the mid-1980s, and they are situated adjacent to each other. In 2013, the stem density was 1242, 1467 and 801 stems·ha⁻¹, and the average leaf area index (*LAI*) was 4.3, 2.3 and 2.0, respectively. The morphological characteristics of the trees, including tree height, diameter at breast height (*DBH*), sapwood width, sapwood area and the total [trunk](#) area at breast height per ground area (A_t/A_G), are presented in Table 1. The forest soil is brunisolic soil with a pH value of 4.0 and a topsoil (0-20 cm) organic carbon content of 15.2-28.2 g·kg⁻¹.

Table 1. Stand and tree morphological characteristics of the experimental plots

Forest type	<i>S. superba</i>	<i>E. citriodora</i>	<i>A. auriculaeformis</i>
Stand age (year)	approx. 30	approx. 30	approx. 30
Investigation plot area	500	250	250
(m²)			
Investigation plot number	3	3	3
Stem density (stems·ha⁻¹)	1242±32	1467±150	801±46
<i>LAI</i>^a	4.3	2.3	2.0
Tree height (m)	12.25±0.18	20.94±1.32	17.68±0.58
<i>DBH</i> (cm)^b	16.37±0.43	19.40±0.94	19.14±1.13
Sapwood width (cm)	6.63±0.17	1.56±0.07	1.78±0.03
Sapwood area (cm²)	230.57±11.68	95.69±8.97	93.27±7.76
A_t/A_G (cm²·m⁻²)^c	29.68±0.31	53.37±0.62	27.58±5.26

^a *LAI*, leaf area index.

^b *DBH*, diameter at breast height.

^c A_t/A_G , the total [trunk](#) area at breast height per ground area.

2.2. Environmental monitoring

A photosynthetically active radiation (*PAR*, μmol·m⁻²·s⁻¹) sensor (Li-Cor Quantum Sensor, Li-Cor, USA), a temperature (*T*,) and humidity (*RH*, %) sensor (HC2-S3,

ROTRONIC, Switzerland) and a wind speed (u , $\text{m}\cdot\text{s}^{-1}$) sensor (AN4, Delta-T, UK) were mounted on the top of an 18 m high observation tower erected in the *S. superba* plantation. Three SM200-05 sensors (SM200-05, Delta-T Device, UK) were buried 30 cm under the soil surface at each stand to detect the volumetric soil water content (SWC , $\text{m}^3\cdot\text{m}^{-3}$). All of the sensors were connected to a data logger (DL2e, Delta-T Devices, UK). The sensors read every 30 s, and the 10-min averaged data were recorded. The vapour pressure deficit (VPD , kPa) was calculated using the following formula (Campbell and Norman, 1998):

$$(1)$$

where a , b and c are fixed parameters (0.611 kPa, 17.502 (unitless) and 240.97, respectively).

Ambient trace gases (NO , NO_2 , SO_2 and O_3) concentrations were monitored and recorded every 10 minutes using Model 42i-TL (for measuring NO and NO_2), Model 43i-TLE (for measuring SO_2) and Model 49i (for measuring O_3) gas analysers (Thermo Fisher Scientific Inc., Massachusetts, USA) after [dehumidification](#). These gas analyzers were installed in a [laboratory building](#) nearly 300 m from the experimental plot. The sample inlets, covered with a gauze filter, were set on the roof of the building and connected to the gas analyzers through Teflon tubes. The measured trace gas concentration represents that above the canopy in the experimental plot. The analysers were calibrated every two weeks using a Model 146i analyser (Thermo Fisher Scientific Inc., Massachusetts, USA).

2.3. Sap flow measurements

In total, 21, 15 and 15 sample trees of different diameter classes were selected in the *S. superba*, *E. citriodora* and *A. auriculaeformis* plantations, respectively, for sap flow measurement. The self-made Granier-type sensors were consisted of a pair of 2 cm

long stainless steel probes containing a fine-wire copper-constantan thermocouple and being set in an aluminium tube for each. These sensors were vertically inserted into the sapwood of the sample trees at breast height (1.3 m above ground) on the northern side of the stem. The two probes of each sensor were installed approximately 10 cm apart. The upper probe was heated by a constant direct current of 120 mA with a power of 0.2 W, and the lower probe remained unheated. A plastic cover was placed over the sensor pair to protect against mechanical damage, and then the plastic cover was wrapped with aluminium foil to prevent rain soaking and direct radiation. The instantaneous temperature difference between the probes was converted into a voltage value and recorded in a data logger (DL2e, Delta-T Devices, UK). The reading was synchronous with that of environmental factors. Finally, the sap flux density (J_s , $\text{g}\cdot\text{m}^{-2}\cdot\text{s}^{-1}$) was calculated according to the following formula (Granier, 1987):

(2)

where ΔT_m is the temperature difference obtained under zero flux conditions, and ΔT is the instantaneous temperature difference. These temperature difference data were converted to sap flux density using the Baseline 3.0 program developed by the Nicholas School of Environment and Earth Sciences at Duke University, USA.

2.4. Calculation of whole-tree transpiration

To avoid damage to sample trees in the experimental plot, we selected 15-20 trees of different diameter classes for each plantation outside the plots and obtained stem core samples using an increment borer. Sapwood width was determined visually from coloration changes between heartwood and sapwood. The diameter at breast height (*DBH*) was directly measured at 1.3 m above the ground by a *DBH* ruler. We established the relationship between the *DBH* (cm) and sapwood area (A_s , cm^2) calculated from the sapwood width as follows:

(3)

where k and b are coefficients obtained through a non-linear regression analysis. The [regression equation](#) for *S. superba*, *E. citriodora* and *A. auriculaeformis* were the following: $A_s=0.61 \times (DBH)^{2.02}$ ($R^2=0.99$), $A_s=0.30 \times (DBH)^{1.88}$ ($R^2=0.97$) and $A_s=1.39 \times (DBH)^{1.41}$ ($R^2=0.98$), respectively. Based on the measured DBH and the established formula, the sapwood area of each tree in each investigation plot was obtained. The whole-tree transpiration (E_t , $g \cdot s^{-1}$) was calculated as follows:

(4)

When using formula (4), the radial variation of J_s should be considered. Because the sapwood width of *E. citriodora* and *A. auriculaeformis* trees in this study is below 3.5 cm, the J_s measured by 2 cm long probes can reflect the average sap flow density on the entire sapwood section. *S. superba* trees usually have a sapwood depth of more than 4 cm, therefore the radial variation of J_s was considered according to a former study conducted by Zhu *et al.* 2012 at the identical site.

2.5. Estimation of canopy stomatal conductance

The canopy stomatal conductance (G_C) was calculated based on a simplified equation (Braun *et al.*, 2010):

(5)

where ρ is the density of water ($998 \text{ kg} \cdot \text{m}^{-3}$), G_v is the universal gas constant adjusted for water vapour ($0.462 \text{ m}^3 \cdot \text{kPa} \cdot \text{K}^{-1} \cdot \text{kg}^{-1}$), and E_L ($\text{m} \cdot \text{s}^{-1}$) is the canopy transpiration per unit of leaf area with consideration to the time lags between sap flux measured on the stem at breast height and the canopy environmental variables. E_L is calculated by dividing the stand transpiration per ground area (E_C , $\text{m} \cdot \text{s}^{-1}$) by the leaf area index (LAI) measured using a LI-2000 plant canopy analyzer (LI-2000, LI-COR, USA)

under diffuse light conditions in June (the *LAI* of the studied forest stands displayed no obvious seasonal change). To convert canopy G_C in $\text{m}\cdot\text{s}^{-1}$ to $\text{mol}\cdot\text{m}^{-2}\cdot\text{s}^{-1}$, the canopy G_C was divided by the density of the water vapour ($\text{m}^3\cdot\text{mol}^{-1}$, $0.0224\times\text{air temp (K)}/273$) according to Renninger *et al.*, (2014). The calculation of E_C has been described in detail by Ma *et al.* (2008). The time lag was calculated using the method provided by Phillips *et al.* (1997).

To reduce errors, the estimation of the daytime mean G_C (from 8:00 to 18:00) was limited to conditions in which $VPD\geq 0.2$ kPa according to Phillips *et al.* (1998) and Tang *et al.* (2006), so was the calculation of the flux of trace gases which was based on the G_C value. Therefore, the days with a [high humidity](#) were excluded. When examining the response of G_C to environmental factors, we used a filter of $VPD=0.6$ kPa to exclude G_C data for $VPD < 0.6$ kPa, as suggested by Ewers and Oren (2000).

2.6. Calculation of canopy uptake of trace gases

The flux of measured trace gases (NO , NO_2 , SO_2 and O_3) into the foliage can be calculated using the following equation (Slovik *et al.*, 1996):

(6)

where F_{gas} is the flux of the gases into the foliage, $[\text{gas}]_a$ is the trace gas concentration in ambient air, $[\text{gas}]_i$ is the intercellular trace gas concentration, and G_{gas} is the canopy stomatal conductance for a given gas. According to Graham's law, when a two-way exchange between two types of gases occurs on an interface, the diffusivity of one gas (D_1) can be estimated by multiplying the known diffusivity of the other gas (D_2) by the square root of the ratio of their molecular masses (Massman 1998; Slovik *et al.*, 1996):

(7)

where M_1 and M_2 are the corresponding molecular masses of the two gases. For the

leaf stomata where the water vapour and trace gases exchange, the diffusivity is the stomatal conductance. Thus, the stomatal conductance for trace gases (G_{gas}) can be calculated using the following equation:

(8)

where is the canopy stomatal conductance for water vapour obtained using equation (5), and the value for NO, NO₂, SO₂ and O₃ was 0.775, 0.626, 0.530 and 0.613, respectively (Slovik *et al.*, 1996). Because the water solubility of SO₂ is high, the intercellular SO₂ concentration within the leaf is considered to be close to zero, namely $[\text{SO}_2]_i=0$; the same is true for ozone (Slovik *et al.*, 1996). By contrast to SO₂ and O₃, the intercellular concentrations of NO and NO₂ are greater than zero. A compensation concentration point should be determined because NO_x can diffuse into the leaf only when its concentration exceeds this point. A few studies suggest a compensation point for NO₂ ranging from 0.1 to 3.2 ppb NO₂ depending on the tree species (Chaparro-Suarez *et al.*, 2011). In this study, we assume the intercellular NO or NO₂ concentration to be 3.2 ppb. Although the actual values of the flux are potentially underestimated or overestimated, this estimation bias is minimal because the NO or NO₂ concentration of the ambient air is significantly higher than the intercellular concentration most of the time.

2.7. Statistical analyses

Statistical analyses were performed by SPSS 17.0 (SPSS Inc., USA). A one-way ANOVA followed by a Duncan's test was used to test for significant differences ($P<0.05$) in atmospheric trace gas concentration among different seasons, daytime mean G_c among different seasons for a given tree species, daytime mean G_c among different tree species for a specific season and flux of trace gases among different seasons for each tree type. Independent sample t-tests were used to examine whether

the differences in daytime mean G_C between the wet and dry season were significant ($P<0.05$) under the similar meteorological condition. These figures were plotted by Origin 8.6 (OriginLab Corp., USA).

Because of a power outage or equipment failure, there existed some missing data. The relationship between the G_C and environmental factors (PAR , VPD and T) was established monthly by a non-linear regression analysis and used to fill the G_C gap.

3. Results and Discussions

3.1. Concentrations of atmospheric trace gases

The annual cycle of daily average concentrations for the studied trace gases (NO , NO_2 , SO_2 and O_3) is shown in Figure 1. The annual mean concentration for NO , NO_2 , SO_2 and O_3 were 18.17, 58.05, 12.76 and 42.36 $\mu g \cdot m^{-3}$, respectively. The annual average NO_2 and NO_x concentrations exceeded the Grade II National Ambient Air Quality Standard (GB3095-2012) (MEP 2012) of 40 $\mu g \cdot m^{-3}$ for NO_2 and 50 $\mu g \cdot m^{-3}$ for NO_x . The seasonal variation of the daily average concentrations is presented in Figure 2 (spring: from Mar. to May, summer: from Jun. to Aug., autumn: from Sep. to Nov., winter: Dec., Jan. and Feb.). The daily average concentrations of oxidized nitrogen (NO and NO_2) in spring and winter were significantly higher than those in summer and autumn ($P<0.05$). For SO_2 , the mean value of the daily average concentrations was the highest in winter and the lowest in summer. However, the O_3 concentration presented a different seasonal pattern. The mean value of the daily average concentrations in autumn was 56.07 $\mu g \cdot m^{-3}$, which was 1.64, 1.39 and 1.45 times of that in the spring, summer and winter, respectively.

Zhang *et al.* (2007) and Van *et al.* (2006) also demonstrated that a maximum NO_2 concentration was found during the wintertime in the eastern part of China because of the prominent anthropogenic activity and the wintertime meteorological conditions

under which NO_x has a longer lifetime. The SO_2 concentration peaks during the winter season, as reported by Wan *et al.* (2011) and Carmichael *et al.* (2003). This peak is likely the result of an increase in the emissions associated with domestic heating and a decrease in the rate of the gas-phase loss of SO_2 via chemical conversion to sulphate in the winter. Additionally, the lower concentration in summer may be associated with the increased precipitation (Carmichael *et al.*, 2003). Higher monthly O_3 values were observed in the early fall (September-October) in Hong Kong (Dufour *et al.*, 2010). Hong Kong is located near our studied site in Guangzhou, therefore, the results of this previous study agreed with our monitoring values. The higher values were attributed to the photochemically generated O_3 from sunshine and the anthropogenic and natural precursors during this period (Tu *et al.*, 2007).

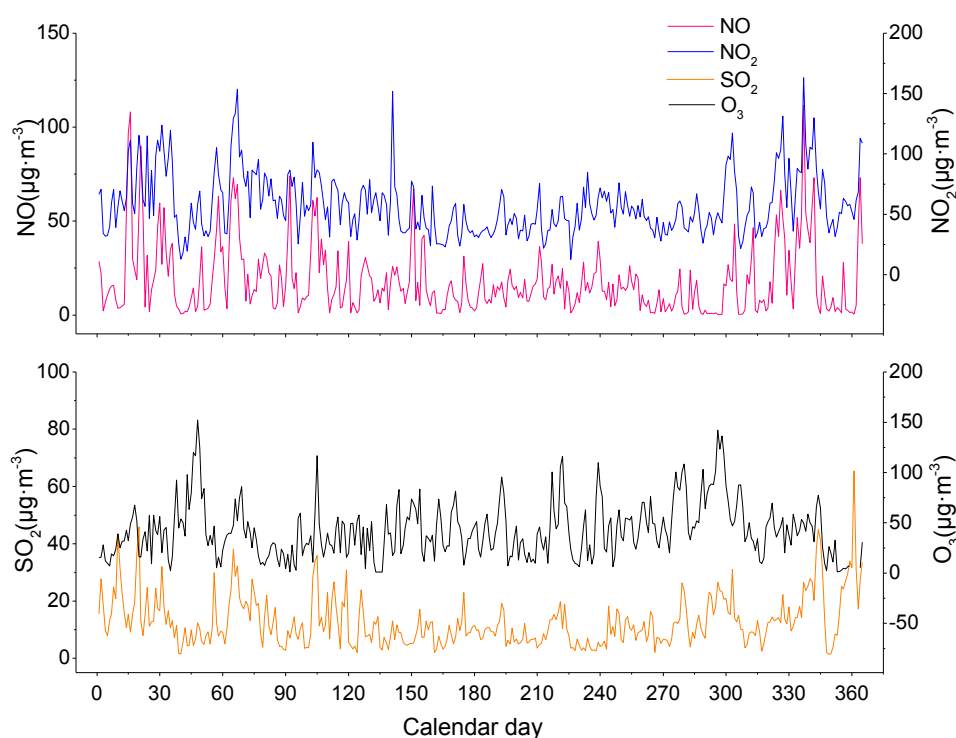


Figure 1. Annual course of daily average concentrations of NO_x , SO_2 and O_3 for 2013

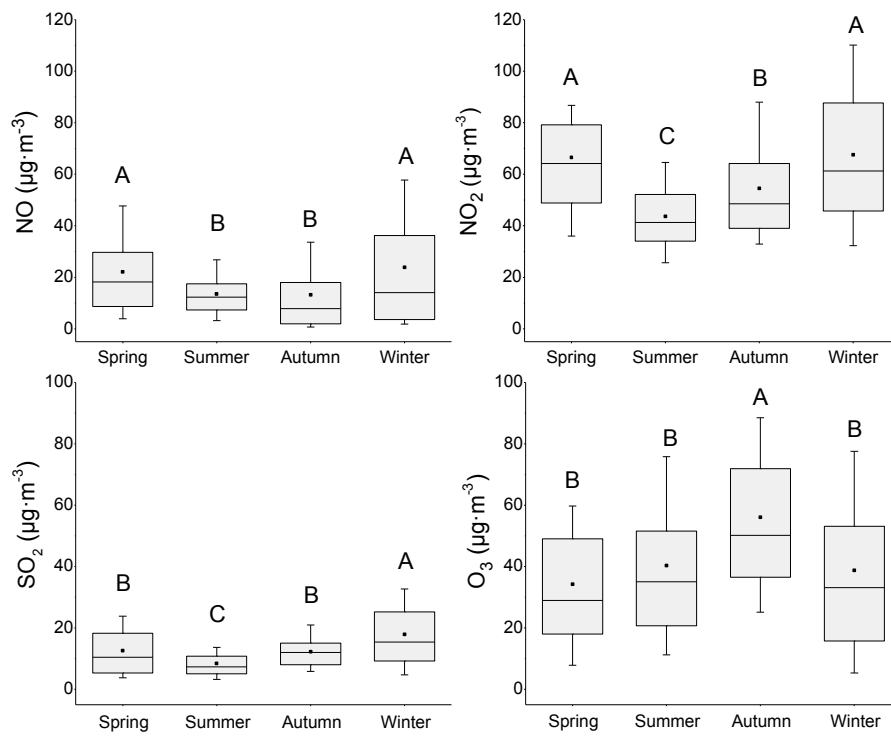


Figure 2. Seasonal variation of daily average concentrations for trace gases in 2013. Different letters indicate significant differences (Duncan's test, $\alpha = 0.05$). Boxes represent 25 and 75 percentiles; the median line and average dot are presented inside. Error bars represent the 10th and 90th percentiles.

3.2. Canopy stomatal conductance and its relationship with environmental factors

Daytime mean G_c (from 8:00 to 18:00) under the condition of $VPD \geq 0.2$ kPa varied with ambient environmental conditions over the annual course (Figure 3). At the seasonal time scale, the daytime mean G_c in summer was significantly higher than those in other seasons in *S. superba* and *E. citriodora* plantations ($P < 0.05$), as shown in Figure 4. For *A. auriculaeformis*, the highest value was observed in the spring followed by the summer, whereas the values in autumn and winter were relatively lower. On a diurnal time scale, two peaks for the G_c were noted on clear sky days in

the wet season: the first peak appeared between 8:00 and 10:00 and the second between 16:00 and 17:00. In the dry season, the G_C reached its maximum around midday and then gradually declined throughout the afternoon, presenting a different pattern from that of the wet season (Figure 5).

Select differences were noted in the daytime mean G_C among the three tree species because of their distinct physiological characteristics (Figure 4). The daytime mean G_C in *S. superba* and *E. citriodora* plantations were significantly higher than that in *A. auriculaeformis* plantation ($P<0.05$) in the summer, autumn and winter. Nevertheless, this relationship was not the case for spring, in which the value in *A. auriculaeformis* plantation showed the highest level.

The G_C value is determined by the sap flux (J_s) and the sapwood area/ leaf area ratio ($A_S: A_L$) according to the method used in this study. Our results showed that the daytime mean G_C in *S. superba* and *E. citriodora* plantations were, respectively, 1.12-1.66 and 1.11-1.43 times that of *A. auriculaeformis* stand in all seasons except for spring, and the $A_S:A_F$ value were 1.52 and 1.60 times that of *A. auriculaeformis* plantation, respectively. Based on the discordant proportional relation for the G_C and $A_S: A_L$, we conclude that the daytime mean G_C in *S. superba* being higher than that in *A. auriculaeformis* was associated with a higher J_s and $A_S: A_F$ in *S. superba*, whereas the higher value in *E. citriodora* compared with that in *A. auriculaeformis* was the consequence of the $A_S: A_F$ alone.

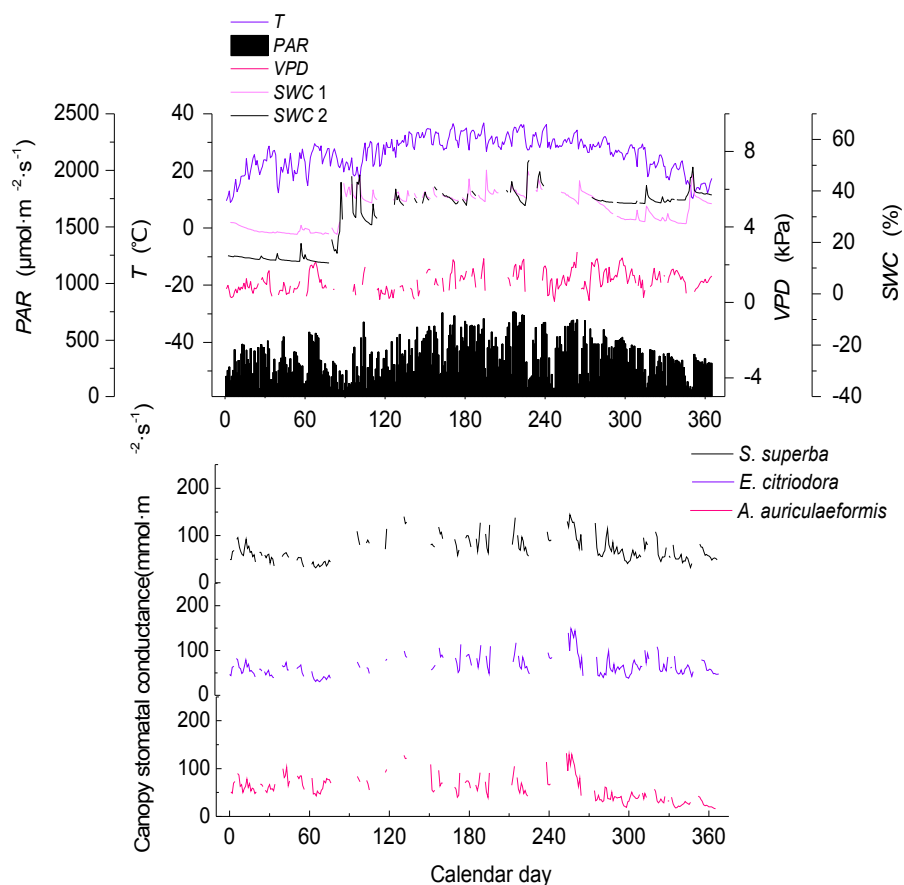


Figure 3. Annual course of environmental factors and daytime mean canopy stomatal conductance for 2013. *SWC1* represents the soil water content at the *S. superba* plot, whereas *SWC2* represents the soil water content at the *E. citriodora* and *A. auriculaeformis* plots.

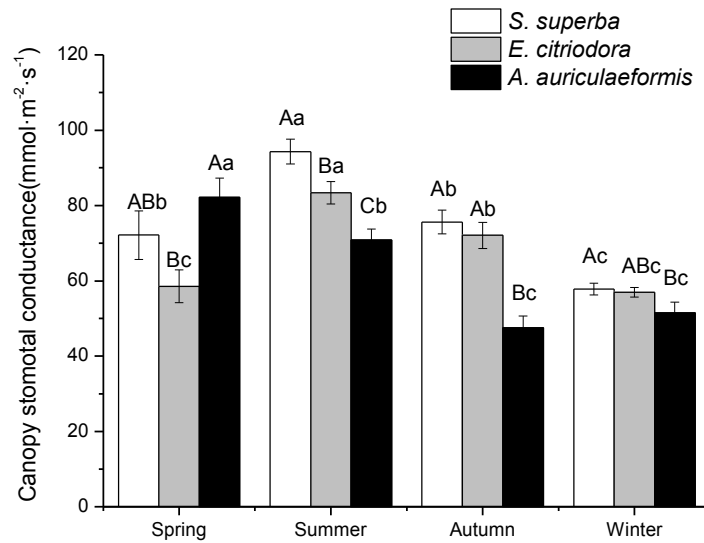


Figure 4. Seasonal variation of daytime mean canopy stomatal conductance for $VPD \geq 0.2$ kPa. Different capital letters indicate significant differences among different tree species for a given season (Duncan's test, $\alpha=0.05$). Different lowercase letters indicate significant differences among different seasons for a given tree species (Duncan's test, $\alpha=0.05$).

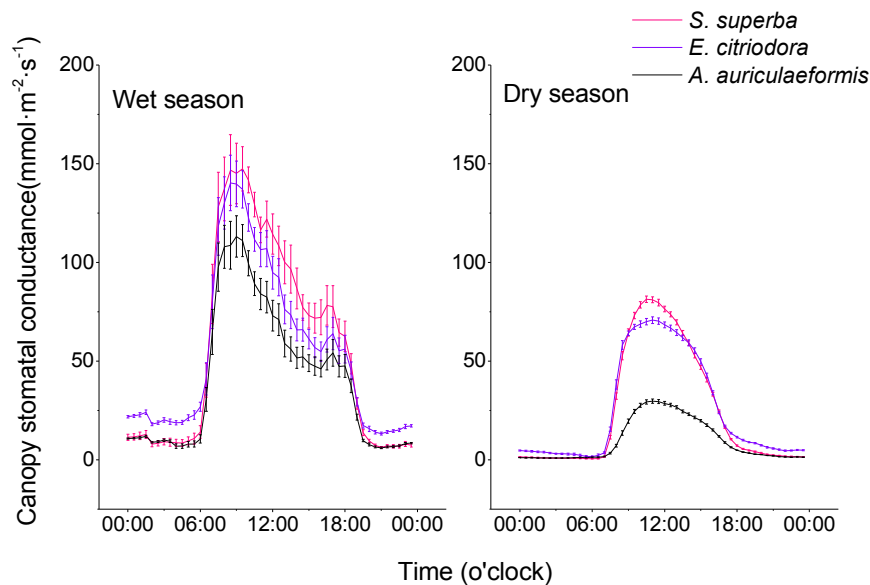


Figure 5. Diurnal variation of canopy stomatal conductance on clear days during wet and dry seasons

As presented in Table 2, a partial correlation analysis shows that the daytime mean G_C was positively correlated with the daytime mean PAR ($P<0.001$) when the VPD was treated as a controlled variable. Unlike the relationship between the G_C and PAR , the daytime mean G_C showed a negative correlation with the daytime mean VPD when PAR served as the controlled variable ($P<0.001$). According to the response of G_C to PAR or VPD mentioned above, a higher G_C value occurred in the case of a higher PAR or lower VPD . However, a positive correlation was noted between the daytime mean PAR and VPD ($P<0.001$) as demonstrated in Figure 6 from the data of the wet and dry seasons (the wet season was from Apr. to Sep. whereas the dry season occurred over the remaining months), indicating non-simultaneous [circumstances](#) of a high PAR with low VPD . Hence, the conditions under which the daytime mean G_C can reach a maximum deserve additional discussion.

Table 2. The partial correlation analysis of the daytime mean G_C and daytime mean PAR or VPD ^a

Forest type	(a) G_C Versus PAR			(b) G_C Versus VPD		
	R	P value	df	R	P value	df
<i>S. superba</i>	0.69	<0.001	127	-0.57	<0.001	127
<i>E. citriodora</i>	0.59	<0.001	128	-0.58	<0.001	128
<i>A. auriculaeformis</i>	0.64	<0.001	128	-0.56	<0.001	128

^a R represents the partial correlation coefficient; df denotes the degree of freedom.

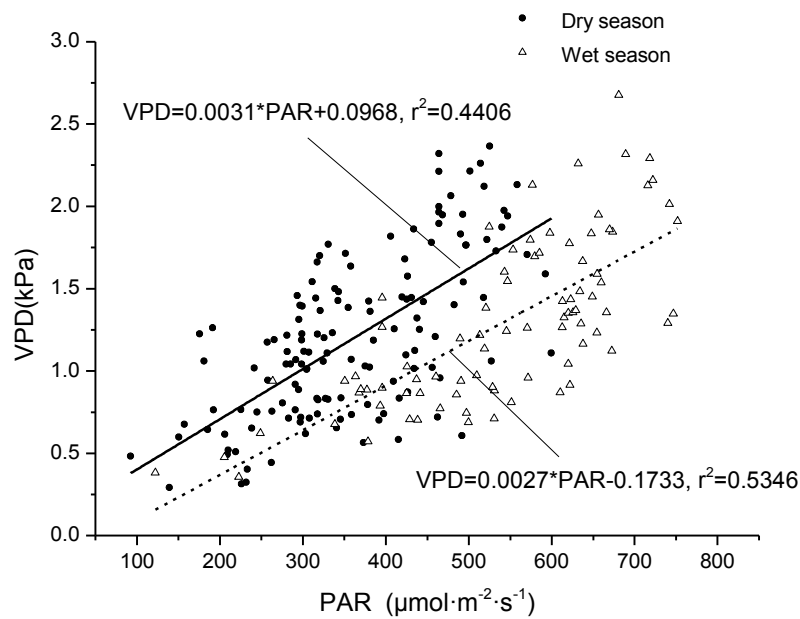


Figure 6. The [linear regression](#) between the daytime mean PAR and VPD .

We plotted the daytime mean G_C against the daytime mean PAR and VPD during the dry and wet seasons (Figure 7). The maximal daytime mean G_C did not appear in concurrence with the highest PAR . In the dry season, the daytime mean G_C reached its maximum when the daytime mean VPD was in the range of 0.7 to 1.0 kPa and the PAR average was between 300 $\mu\text{mol}\cdot\text{m}^{-2}\cdot\text{s}^{-1}$ and 400 $\mu\text{mol}\cdot\text{m}^{-2}\cdot\text{s}^{-1}$. During the wet season, the daytime mean G_C maxima occurred when the VPD ranged between 0.8 kPa and 1.1 kPa and the PAR average appeared from 450 to 550 $\mu\text{mol}\cdot\text{m}^{-2}\cdot\text{s}^{-1}$. Therefore, the G_C value was synergistically regulated by the PAR and VPD . The G_C began to decrease when the VPD was above a threshold, as reported in previous studies (Gerosa *et al.*, 2008, Ghimire *et al.*, 2014, Wang *et al.*, 2012). The VPD threshold was 1.8-2.1 kPa for *Fagus sylvatica* L. and *Quercus robur* L. in South Alpine environmental condition (Gerosa *et al.*, 2008) and was 0.4 kPa for a natural broad-leaved forest and a planted coniferous forest in Central Nepal (Ghimire *et al.*,

2014), whereas the value in this study was between 0.7 kPa and 1.1 kPa. The VPD threshold varies with plant species and environmental condition, which may result from the longtime adaption to the surrounding environment (Gerosa *et al.*, 2008).

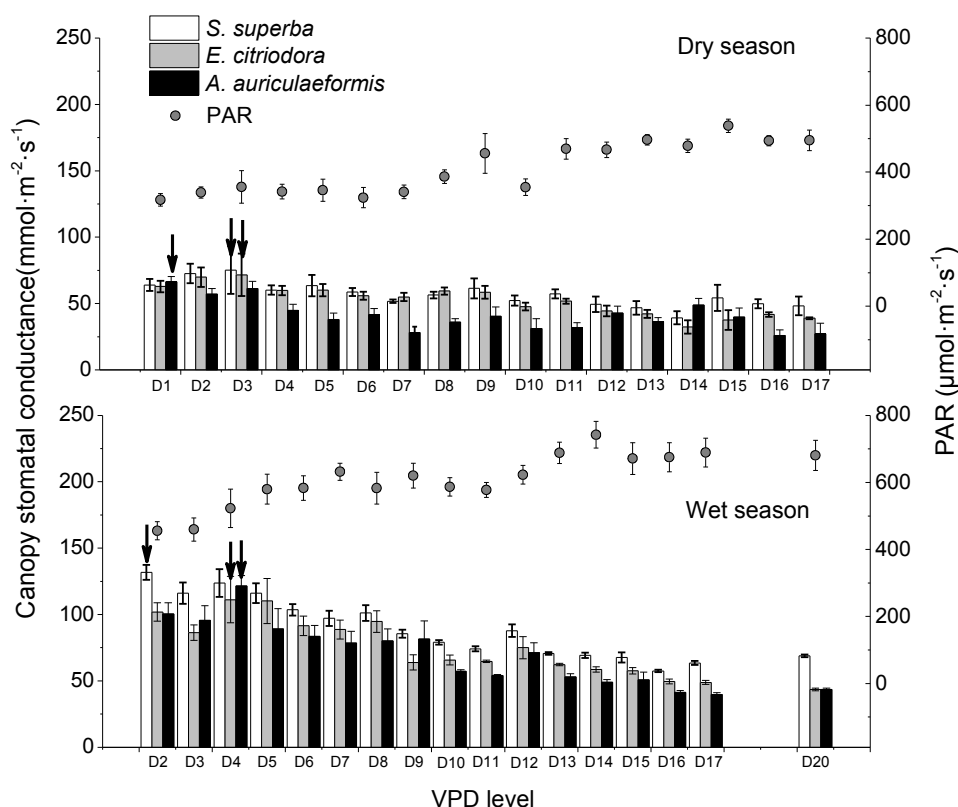


Figure 7. Variation in the daytime mean G_C under the influence of meteorological factors during the dry and wet seasons. The arrows indicate the maximal daytime mean G_C . The VPD value was sorted at intervals of 0.1 kPa beginning with 0.7 kPa, i.e., $D1$ represents the VPD range of 0.7 to 0.8 kPa, $D2$ represents that of 0.8-0.9 kPa, and the VPD range of the following $D3$ to $D20$ can be determined using the same reckoning.

PAR and VPD are important factors influencing stomatal behaviour and constraining G_C to its maximal value, as demonstrated above. However, the [respective restriction](#) effect of the PAR or VPD on G_C needed to be analysed separately. By

processing the data when the SWC exceeded $0.30 \text{ m}^3 \cdot \text{m}^{-3}$, we found a negative logarithmical relationship between the daytime mean G_c and VPD when the PAR was in the same range ($400\text{-}600 \text{ }\mu\text{mol} \cdot \text{m}^{-2} \cdot \text{s}^{-1}$) (Figure 8). The relationship was described with the following fitting equation: ($P<0.001$). In contrast, the daytime mean G_c was positively and logarithmically related with the PAR under four VPD levels: (a and b values are listed in Table 3) ($P<0.01$). Because the differential coefficient () of the equation for the relation between the G_c and PAR declined with the increased PAR , the increase extent of the daytime mean G_c was larger with the same PAR increase magnitude at lower PAR levels. This relationship suggests that PAR played a more significant role in regulating stomatal behaviour at low PAR levels.

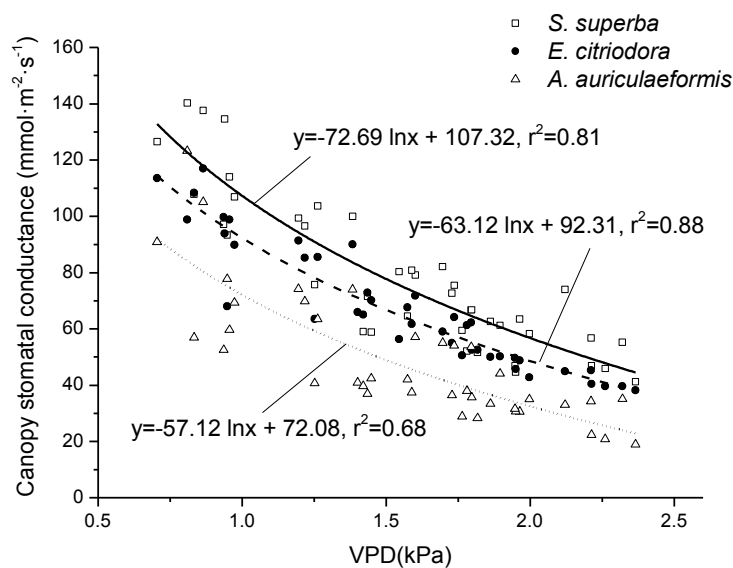


Figure 8. The response of the daytime mean G_c to the VPD under the identical PAR range.

Table 3. Response of the daytime mean G_c to the PAR under different VPD levels ^a

VPD (kPa)	$S. superba$			$E. citriodora$			$A. auriculaeformis$		
	a	b	r^2	a	b	r^2	a	b	r^2
1.0-1.2	67.35	322.42	0.87	47.10	205.40	0.58	59.87	306.32	0.60
1.2-1.4	43.48	188.64	0.71	28.56	103.53	0.69	42.03	206.34	0.69

1.4-1.6	50.81	241.75	0.90	23.82	79.74	0.50	46.90	244.15	0.77
1.6-1.8	48.22	232.68	0.81	22.83	83.30	0.54	55.79	304.53	0.80

^a The a and b are coefficients obtained by a non-linear regression analysis: $y = a \cdot x^b$. The letter r indicates the Pearson correlation coefficient.

Apart from the *PAR* and *VPD*, the soil water content (*SWC*) affects the physiological activity of plants (stomatal opening) (Zimmermann *et al.*, 2006). Unlike the *PAR* and *VPD* which exerted an effect at a relatively short timescale, the effect of *SWC* would be significant on a longer timescale such as a monthly or seasonal timescale. According to [synchronous](#) measurements of the *SWC* in this research, the average *SWC* value during the wet season ($0.38 \text{ m}^3 \cdot \text{m}^{-3}$ in the *S. superba* plantation and $0.37 \text{ m}^3 \cdot \text{m}^{-3}$ in both the *E. citriodora* and *A. auriculaeformis* plantations) was significantly higher than that in the dry season ($0.29 \text{ m}^3 \cdot \text{m}^{-3}$ in the *S. superba* plantation and $0.26 \text{ m}^3 \cdot \text{m}^{-3}$ in both the *E. citriodora* and *A. auriculaeformis* plantations) ($P < 0.05$). Corresponding to the *SWC* seasonal pattern, the daytime mean G_c in the wet season showed a higher value compared to that in the dry season ($P < 0.05$) under the similar *PAR* and *VPD* condition (Figure 9), displaying the significant effects of the *SWC* on the performance of the stomata. A similar response of the G_c to *SWC* has been reported by Ewers *et al.* (2001) and Schäfer 2011. To increase the canopy stomatal conductance and thus enhance the [absorption capacity](#) for trace gases, maintaining a suitable *SWC* may be an [appropriate](#) approach because of the influence of the *SWC* on the behaviour of the stomata and the fact that *SWC* is an [artificially](#) adjustable factor when compared to [meteorological factors](#) (such as the *PAR* and *VPD*).

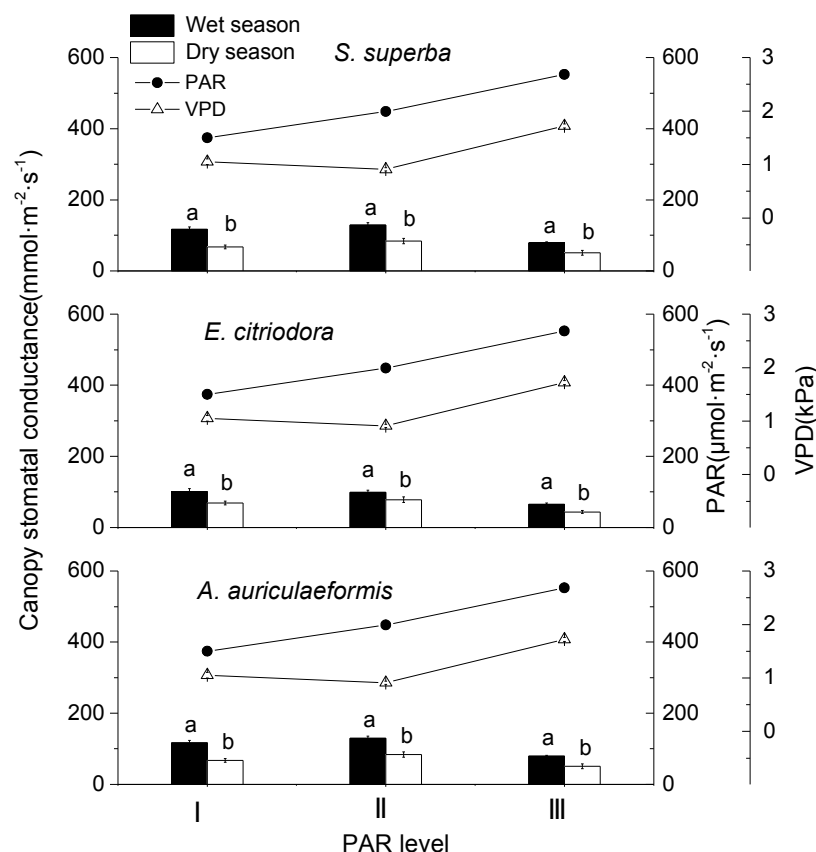


Figure 9. Daytime mean G_c differences between the wet and dry season under three diverse meteorological conditions. Different letters indicate significant differences (Independent sample t test, $\alpha = 0.05$). I, II and III represent the following PAR ranges: 300-400, 400-500 and 500-600 $\mu\text{mol}\cdot\text{m}^{-2}\cdot\text{s}^{-1}$, respectively.

3.3. Fluxes of trace gases

The annual pattern for the daytime mean flux of the four studied trace gases is shown in Figure 10. The combination of the canopy stomatal conductance and the atmospheric concentrations produces fluxes of trace gases. Thus, differences in the seasonal pattern of the canopy stomatal conductance and atmospheric concentrations may result in differentiated peak fluxes. The daytime mean flux for NO, NO₂ and SO₂ exhibited a spring maximum for the three tree species, whereas the daytime mean flux maxima for O₃ occurred in the autumn or summer (Figure 11).

That the flux is not synchronous with the canopy stomatal conductance (or the deposition velocity) or the atmospheric concentration has been demonstrated by previous studies. Zimmermann *et al.* (2006) observed that the flux maxima occurred during October to December for both SO₂ and NO₂ in the eastern Erzgebirge whereas the deposition velocity showed the highest values from May to September when using a modelling method. Wieser *et al.* (2006) reported that the O₃ uptake in a pine forest in Tenerife showed no clear seasonal trend although the ambient ozone concentration showed an obvious seasonal change when using the identical method. This [asynchronism](#) can be attributed to the coincidence of higher O₃ levels with the time when trees suffered from water stresses and the stomata were closed.

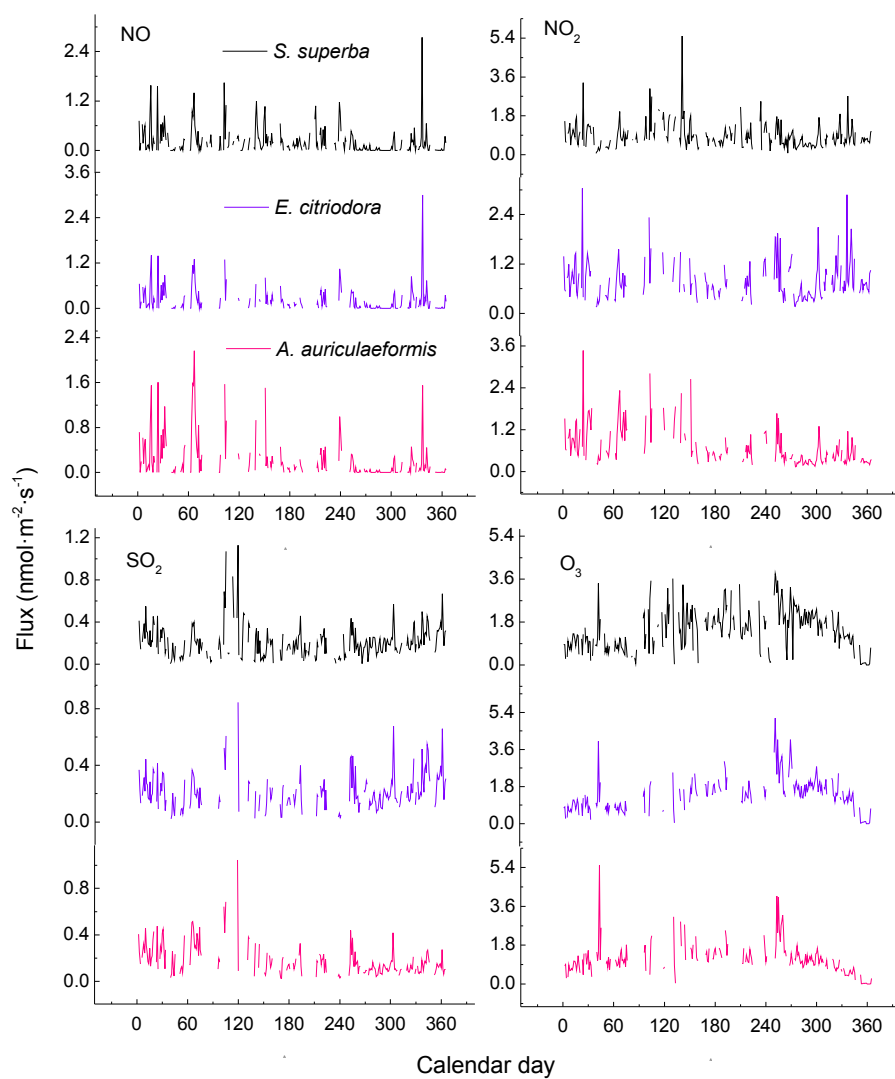


Figure 10. Annual changes in the daytime average fluxes for trace gases.

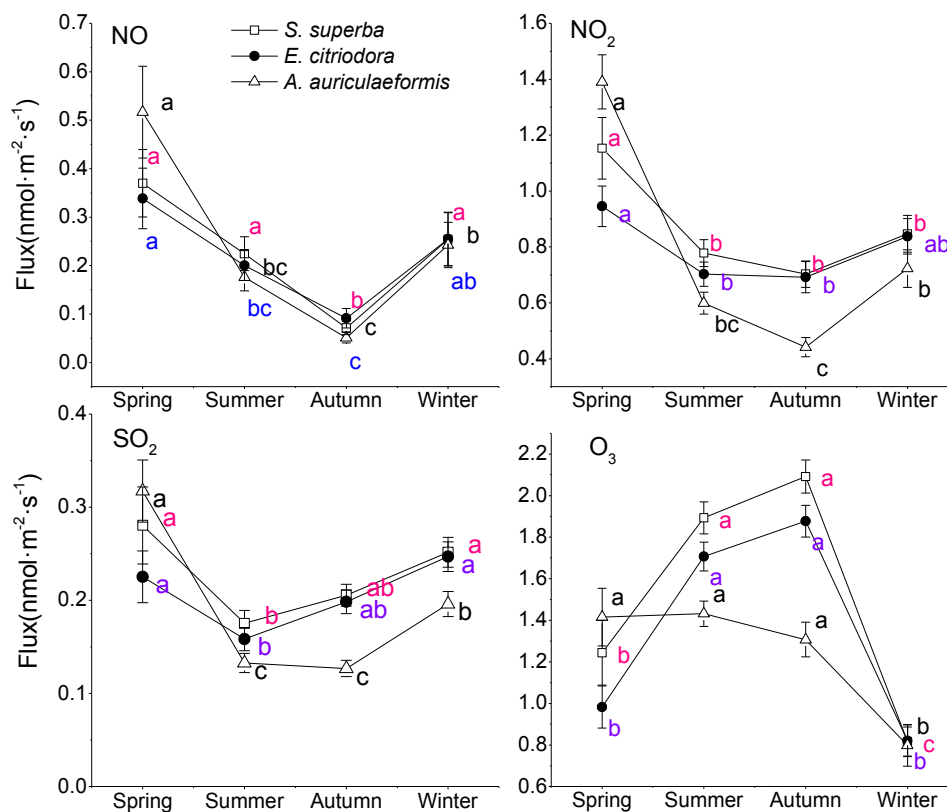


Figure 11. Seasonal variation of daytime average fluxes for trace gases for $VPD \geq 0.2$ kPa. Different letters indicate significant differences among different seasons for a given tree species (Duncan's test, $\alpha=0.05$).

The annual accumulative stomatal flux of NO, NO₂, SO₂ and O₃ were 100.19 ± 3.76 , 510.68 ± 24.78 , 748.59 ± 52.81 and 151.98 ± 9.33 mg·m⁻²·a⁻¹, respectively (Figure 12). The calculated annual accumulative flux was underestimated because the estimation of flux was excluded when $VPD < 0.2$ kPa. Nevertheless, this estimation bias is minimal because the flux is small when $VPD < 0.2$ kPa. Jim and Chen (2008) demonstrated that the removal rate for NO₂ and SO₂ was 3.38 g·m⁻²·a⁻¹ and 2.02 g·m⁻²·a⁻¹, respectively, when analysing the data for 2000 at the identical district. The accumulative uptake was higher in their study because their calculated flux included both the stomatal and non-stomatal uptakes of leaves, whereas only the stomatal flux was estimated in our study. In the next place, the flux was calculated as the product of

the deposition velocity and the concentration of air pollutants in their study, where the deposition velocity was determined as an average value according to the results of other studies rather than a measured value through experiments, this calculation method may result in an imprecise estimation. Additionally, because of the reduction of SO₂ emissions in the PRD region, the ambient SO₂ concentration has decreased during recent years (Fang *et al.*, 2013). Thus, the lower ambient SO₂ concentration in our study may be responsible for the lower cumulative SO₂ uptake as well.

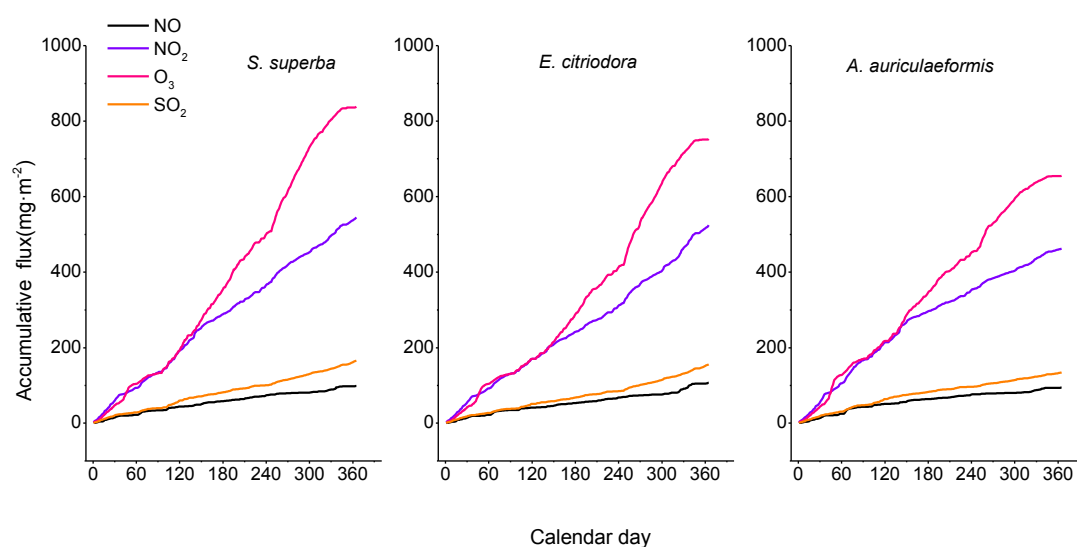


Figure 12. Accumulative stomatal flux of trace gases

3.4. Effects of trace gases on the urban tree canopy

These four trace gases are potential risk constituents in the atmosphere that may exert negative effects on vegetation. We use the exposure-based approach or flux-based approach to assess whether the present levels of these gases had reached a contamination degree, namely the corresponding threshold value. With consideration to the relative sensitivity of different tree species, the SO₂ critical level for a broadleaf forest is assumed to be an annual average of 25 $\mu\text{g}\cdot\text{m}^{-3}$ according to the report of Tao

and Feng (2000). In this present study, the annual average SO_2 concentration was $12.77 \mu\text{g}\cdot\text{m}^{-3}$, nearly half of the critical level, indicating that the present SO_2 concentration had not yet reached the injury level. For NO_2 , the calculated annual average concentration ($58.06 \mu\text{g}\cdot\text{m}^{-3}$) exceeded the critical concentration levels for NO_2 ($30 \mu\text{g}\cdot\text{m}^{-3}$) (De Vries *et al.*, 2000), implying a possibility of NO_2 damage to vegetation. Nevertheless, whether the present NO_2 concentration negatively affected the vegetation requires further study because of the diverse sensitivity of different plants to NO_2 (Kohno *et al.*, 2005).

Two types of approaches have been previously used when assessing the risk of O_3 damage to vegetation. One method is the AOTX index (accumulated exposure over threshold of X ppb). The second method is the $\text{AF}_{\text{st}}\text{Y}$ approach (accumulated stomatal flux over threshold of Y $\text{nmol}\cdot\text{m}^{-2}\cdot\text{s}^{-1}$), this approach entails an estimate of the amount of O_3 entering vegetation via the leaf stoma (Simpson *et al.*, 2007). We calculated the typical AOT40 and $\text{AF}_{\text{st}}1.6$. The AOT40 of the wet season (from Apr. to Sep.) at our study site was $13.13 \text{ ppm}\cdot\text{h}$ (Table 4), exceeding the current European critical level for ozone effects on forest trees ($5 \text{ ppm}\cdot\text{h}$) (UNECE 2004) and even the previous critical level ($10 \text{ ppm}\cdot\text{h}$) (Kärenlampi *et al.*, 1996). In contrast, the $\text{AF}_{\text{st}}1.6$ values for all of the studied species were below $4 \text{ mmol}\cdot\text{m}^{-2}$, the current flux based critical level for O_3 effects on trees (UNECE 2004). The situation during the dry season was similar to that in the wet season, i.e., with an AOT40 above the critical level and an $\text{AF}_{\text{st}}1.6$ below the critical level. Although the estimation of the flux was excluded when $\text{VPD}<0.2 \text{ kPa}$, the calculated $\text{AF}_{\text{st}}1.6$ is credible because the possibility that the flux was above $1.6 \text{ nmol}\cdot\text{m}^{-2}\cdot\text{s}^{-1}$ when $\text{VPD}<0.2 \text{ kPa}$ was small due to the low transpiration, stomatal conductance and O_3 concentration (The generation of O_3 is closely related to the solar radiation intensity (Tu *et al.*, 2007) which is usually low

when the VPD is low).

Only the O_3 molecules that enter the leaves through the stomata are harmful to plants (Fuhrer, 2000). Although the atmospheric O_3 concentration was relatively high based on the AOT40 value, the O_3 had not yet reached the injury level according to the $AF_{st1.6}$ value. Therefore, the performance of the stomata, which is associated with the environmental factors and tree physiological properties, must be considered when analyzing O_3 damage to vegetation. Namely, the flux-based measurement is better suited for evaluating the risk of O_3 impacts on trees than the exposure-based method, as demonstrated in previous studies (Gerosa *et al.*, 2008; Wang *et al.*, 2012). In addition, despite the fact that the AOT40 in the dry season was higher than that in the wet season, the F_{O_3} and $AF_{st1.6}$ exhibited a higher value in the wet season. The relatively lower G_C and the high O_3 concentration not coinciding with the higher stomatal conductance during the dry season were responsible for this [inconsistency](#).

Table 4. Average daytime canopy O_3 uptake rate, AOT40 and $AF_{st1.6}$ estimated during the wet and dry season

Forest type	(a) Wet season			(b) Dry season			
	AOT40	$AF_{st1.6}$	F_{O_3}	AOT40	$AF_{st1.6}$		
		$nmol \cdot m^{-2} \cdot s^{-1}$	$ppm \cdot h$	$mmol \cdot m^{-2}$	$nmol \cdot m^{-2} \cdot s^{-1}$	$ppm \cdot h$	$mmol \cdot m^{-2}$
<i>S. superba</i>		2.05 ± 0.09	13.13	3.95	1.12 ± 0.06	16.22	1.49
<i>E. citriodora</i>		1.92 ± 0.11	13.13	2.99	1.14 ± 0.06	16.22	1.23
<i>A. auriculaeformis</i>		1.64 ± 0.08	13.13	2.37	0.92 ± 0.05	16.22	0.88

4. Conclusions

In this study, we investigated the stomatal uptake of NO_x , SO_2 and O_3 by mature urban plantations (*S. superba*, *E. citriodora* and *A. auriculaeformis*) using the sap flow-based approach in Guangzhou in the PRD region, China. At this study site, the atmospheric concentration exhibited a spring or winter maximum for NO , NO_2 and SO_2 , whereas the concentration maxima for O_3 occurred in the autumn. The canopy

stomatal conductance was jointly regulated by the *PAR* and *VPD*. Apart from the *PAR* and *VPD*, the *SWC* affects the physiological activity of plants. The daytime mean G_c declined with the reduction of the *SWC* under similar meteorological condition. A [comprehensive](#) understanding of the influence pattern of environmental factors on the canopy stomatal conductance could provide references for enhancing the tree canopy capacity to remove trace gases.

Differences in the seasonal pattern of canopy stomatal conductance and atmospheric concentrations led to a differentiated peak flux. The flux for NO, NO₂ and SO₂ exhibited a spring maximum, whereas the flux maxima for O₃ appeared in the autumn or summer. The annual accumulative stomatal flux of NO, NO₂, SO₂ and O₃ was 100.19 ± 3.76 , 510.68 ± 24.78 , 748.59 ± 52.81 and $151.98 \pm 9.33 \text{ mg} \cdot \text{m}^{-2} \cdot \text{a}^{-1}$, respectively. These trace gases had not yet reached the injury level, except for NO₂. Nevertheless, whether the present NO₂ concentration negatively affected the vegetation requires further research because of the diverse sensitivity of different tree species to NO₂. The inconsistent results of the AOT40 and AF_{st}1.6, namely the AOT40 was above the critical level whereas the AF_{st}1.6 was below the critical level, suggested that the flux-based measurement was better suited for evaluating the risk of O₃ effects than the exposure-based method. When we focus on the foliar uptake of trace gases, the effect of these gases on the vegetation in turn should be considered, particularly for regions with serious air pollution problems.

Acknowledgments

This work was supported by the National Natural Science Foundation of China (No. 41275169 and No. 31300335) and Natural Science Foundation of Guangdong Province of China (No. 2014A030313762).

References

- Ainsworth, E.A., Yendrek, C.R., Sitch, S., Collins, W.J. and Emberson, L.D., 2012. The Effects of Tropospheric Ozone on Net Primary Productivity and Implications for Climate Change. *Annual review of plant biology* 63, 637-661.
- Bowman, C.T., 1992. Control of combustion-generated nitrogen oxide emissions: technology driven by regulation. *Symposium (International) on Combustion* 24, 859-878. Elsevier.
- Braun, S., Schindler, C. and Leuzinger, S., 2010. Use of sap flow measurements to validate stomatal functions for mature beech (*Fagus sylvatica*) in view of ozone uptake calculations. *Environmental Pollution* 158, 2954-2963.
- Campbell, G.S. and Norman, J.M., 1998. An introduction to environmental biophysics. Springer.
- Carmichael, G.R. et al., 2003. Measurements of sulfur dioxide, ozone and ammonia concentrations in Asia, Africa, and South America using passive samplers. *Atmospheric Environment* 37, 1293-1308.
- Chaparro-Suarez, I.G., Meixner, F.X. and Kesselmeier, J., 2011. Nitrogen dioxide (NO₂) uptake by vegetation controlled by atmospheric concentrations and plant stomatal aperture. *Atmospheric Environment* 45, 5742-5750.
- De Vries, W., Reinds, G.J., Klap, J.M., Van Leeuwen, E.P. and Erisman, J.W., 2000. Effects of environmental stress on forest crown condition in Europe. Part III, Estimation of critical deposition and concentration levels and their exceedances. *Water, Air, and Soil Pollution* 119, 363-386.
- Dufour, G., Eremenko, M., Orphal, J. and Flaud, J.M., 2010. IASI observations of seasonal and day-to-day variations of tropospheric ozone over three highly populated areas of China, Beijing, Shanghai, and Hong Kong. *Atmospheric Chemistry and Physics* 10, 3787-3801.
- Eichert, T. and Fernández, V., 2012. Uptake and release of elements by leaves and other aerial plant parts. *Marschner's Mineral Nutrition of Higher Plants* 3, 71-84. [Elsevier](#).
- Ewers, B.E. and Oren, R., 2000. Analyses of assumptions and errors in the calculation of

stomatal conductance from sap flux measurements. *Tree Physiology* 20, 579-589.

Ewers, B.E., Oren, R., Phillips, N., Strömberg, M. and Linder, S., 2001. Mean canopy stomatal conductance responses to water and nutrient availabilities in *Picea abies* and *Pinus taeda*. *Tree Physiology* 21, 841-850.

Fang, Y. et al., 2013. Three-decade changes in chemical composition of precipitation in Guangzhou city, southern China, has precipitation recovered from acidification following sulphur dioxide emission control? *Tellus B*, 65.

Fuhrer, J., 2000. Introduction to the special issue on ozone risk analysis for vegetation in Europe. *Environmental Pollution* 109, 359-360.

Gerosa, G., Marzuoli, R., Desotgiu, R., Bussotti, F. and Ballarin-Denti, A., 2008. Visible leaf injury in young trees of *Fagus sylvatica* L. and *Quercus robur* L. in relation to ozone uptake and ozone exposure. An Open-Top Chambers experiment in South Alpine environmental conditions. *Environmental pollution* 152, 274-284.

Ghimire, C.P., Lubczynski, M.W., Bruijnzeel, L.A. and Chavarro-Rincón, D., 2014. Transpiration and canopy conductance of two contrasting forest types in the Lesser Himalaya of Central Nepal. *Agricultural and Forest Meteorology* 197, 76-90.

Grünhage, L., Haenel, H.D. and Jäger, H.J., 2000. The exchange of ozone between vegetation and atmosphere, micrometeorological measurement techniques and models. *Environmental Pollution* 109, 373-392.

Granier, A., 1987. Evaluation of transpiration in a Douglas-fir stand by means of sap flow measurements. *Tree physiology* 3, 309-320.

Jim, C.Y. and Chen, W.Y., 2008. Assessing the ecosystem service of air pollutant removal by urban trees in Guangzhou (China). *Journal of Environmental Management* 88, 665-676.

Josipovic, M., Annegarn, H.J., Kneen, M.A., Pienaar, J.J. and Piketh, S.J., 2010. Concentrations, distributions and critical level exceedance assessment of SO₂, NO₂ and O₃ in South Africa. *Environmental monitoring and assessment* 171, 181-196.

Kärenlampi, L. and Skärby, L., 1996. Critical Levels for Ozone in Europe: Testing and

Finalizing the Concepts .University of Kuopio.

Köstner, B. et al., 2008. Sap flow measurements as a basis for assessing trace-gas exchange of trees. *Flora-Morphology, Distribution, Functional Ecology of Plants* 203, 14-33.

Karl, T.R. and Trenberth, K.E., 2003. Modern global climate change. *Science* 302, 1719-1723.

Karlsson, P.E. et al., 2004. New critical levels for ozone effects on young trees based on AOT40 and simulated cumulative leaf uptake of ozone. *Atmospheric Environment* 38, 2283-2294.

Kohno, Y., Matsumura, H., Ishii, T. and Izuta, T., 2005. Plant responses to air pollution and global change: Establishing critical levels of air pollutants for protecting East Asian vegetation—a challenge. *Plant responses to air pollution and global change*, 243-250. Springer Japan.

Löw, M. et al., 2012. Multivariate analysis of physiological parameters reveals a consistent O₃ response pattern in leaves of adult European beech (*Fagus sylvatica*). *New Phytologist* 196, 162-172.

Liu, Y. et al., 2008. Volatile organic compound (VOC) measurements in the Pearl River Delta (PRD) region, China. *Atmospheric Chemistry and Physics* 8, 1531-1545.

Lu, Q. et al., 2013. Emission trends and source characteristics of SO₂, NO_x, PM₁₀ and VOCs in the Pearl River Delta region from 2000 to 2009. *Atmospheric Environment* 76, 11-20.

Ma, L. et al., 2008. Diurnal, daily, seasonal and annual patterns of sap-flux-scaled transpiration from an *Acacia mangium* plantation in South China. *Annals of forest science* 65, 1-1.

Massman, W.J., 1998. A review of the molecular diffusivities of H₂O, CO₂, CH₄, CO, O₃, SO₂, NH₃, N₂O, NO, and NO₂ in air, O₂ and N₂ near STP. *Atmospheric Environment* 32, 1111-1127.

Matyssek, R. et al., 2004. Comparison between AOT40 and ozone uptake in forest trees of different species, age and site conditions. *Atmospheric Environment* 38, 2271-2281.

- MEP (Ministry of Environmental Protection), 2012. China National Ambient Air Quality Standard(GB3095-2012)
(<http://kjs.mep.gov.cn/hjbhzb/bzwb/dqhjbh/dqhjzlbz/201203/W020120410330232398521.pdf>)
- Nunn, A.J. et al., 2007. Exemplifying whole-plant ozone uptake in adult forest trees of contrasting species and site conditions. *Environmental Pollution* 146, 629-639.
- Phillips, N., Nagchaudhuri, A., Oren, R. and Katul, G., 1997. Time constant for water transport in loblolly pine trees estimated from time series of evaporative demand and stem sapflow. *Trees* 11, 412-419.
- Phillips, N. and Oren, R., 1998. A comparison of daily representations of canopy conductance based on two conditional time-averaging methods and the dependence of daily conductance on environmental factors. *Annales des Sciences Forestieres* 55, 217-235. EDP Sciences.
- Pleim, J.E., Finkelstein, P.L., Clarke, J.F. and Ellestad, T.G., 1999. A technique for estimating dry deposition velocities based on similarity with latent heat flux. *Atmospheric Environment* 33, 2257-2268.
- Ramanathan, V., Cicerone, R.J., Singh, H.B. and Kiehl, J.T., 1985. Trace gas trends and their potential role in climate change. *Journal of Geophysical Research* 90, 5547-5566.
- Renninger, H.J., Carlo, N., Clark, K.L. and Schäfer, K.V.R., 2014. Physiological strategies of co-occurring oaks in a water-and nutrient-limited ecosystem. *Tree physiology*, tpt122.
- Richter, A., Burrows, J.P., Nüß, H., Granier, C. and Niemeier, U., 2005. Increase in tropospheric nitrogen dioxide over China observed from space. *Nature* 437, 129-132.
- Schäfer, K.V.R., 2011. Canopy stomatal conductance following drought, disturbance, and death in an upland oak/pine forest of the New Jersey Pine Barrens, USA. *Frontiers in plant science* 2.
- Schulze, E.-D. et al., 2010. The European carbon balance. Part 4, integration of carbon and other trace - gas fluxes. *Global Change Biology* 16, 1451-1469.

- Seinfeld, J.H. and Pandis, S.N., 2012. Atmospheric chemistry and physics: from air pollution to climate change. John Wiley & Sons.
- Setälä, H., Viippola, V., Rantalainen, A.-L., Pennanen, A. and Yli-Pelkonen, V., 2013. Does urban vegetation mitigate air pollution in northern conditions? Environmental Pollution 183, 104-112.
- Simpson, D., Ashmore, M.R., Emberson, L. and Tuovinen, J.P., 2007. A comparison of two different approaches for mapping potential ozone damage to vegetation. A model study. Environmental Pollution 146, 715-725.
- Slovik, S., Siegmund, A., FÜHrer, H.W. and Heber, U., 1996. Stomatal uptake of SO₂, NO_x and O₃ by spruce crowns (*Picea abies*) and canopy damage in Central Europe. New phytologist 132, 661-676.
- Smith, S.J. et al., 2011. Anthropogenic sulfur dioxide emissions, 1850–2005. Atmospheric Chemistry and Physics 11, 1101-1116.
- Sparks, J.P., 2009. Ecological ramifications of the direct foliar uptake of nitrogen. Oecologia 159, 1-13.
- Tang, J. et al., 2006. Sap flux–upscaled canopy transpiration, stomatal conductance, and water use efficiency in an old growth forest in the Great Lakes region of the United States. Journal of Geophysical Research, Biogeosciences (2005–2012) 111.
- Tao, F. and Feng, Z., 2000. Critical loads of SO₂ dry deposition and their exceedance in south China. Water, air, and soil pollution 124, 429-438.
- Tu, J., Xia, Z.-G., Wang, H. and Li, W., 2007. Temporal variations in surface ozone and its precursors and meteorological effects at an urban site in China. Atmospheric Research 85, 310-337.
- UNECE, 2004. Manual on methodologies and criteria for modelling and mapping critical loads and levels and air pollution effects, risks and trends. (<http://www.icpmapping.org>)
- Vahedpour, M. and Zolfaghari, F., 2011. Mechanistic study on the atmospheric formation of acid rain base on the sulfur dioxide. Structural Chemistry 22, 1331-1338.

- Van der A, R.J. et al., 2006. Detection of the trend and seasonal variation in tropospheric NO₂ over China. *Journal of Geophysical Research, Atmospheres* (1984–2012) 111.
- Wan, J.-M. et al., 2011. Change of air quality and its impact on atmospheric visibility in central-western Pearl River Delta. *Environmental monitoring and assessment* 172, 339-351.
- Wang, H. et al., 2012. Ozone uptake by adult urban trees based on sap flow measurement. *Environmental Pollution* 162, 275-286.
- Wang, T., Poon, C.N., Kwok, Y.H. and Li, Y.S., 2003. Characterizing the temporal variability and emission patterns of pollution plumes in the Pearl River Delta of China. *Atmospheric Environment* 37, 3539-3550.
- Wang, T. et al., 2009. Increasing surface ozone concentrations in the background atmosphere of Southern China, 1994–2007. *Atmospheric Chemistry and Physics* 9, 6217-6227.
- Wang, X. et al., 2013. Reductions in sulfur pollution in the Pearl River Delta region, China, Assessing the effectiveness of emission controls. *Atmospheric Environment* 76, 113-124.
- Wieser, G., Luis, V.C. and Cuevas, E., 2006. Quantification of ozone uptake at the stand level in a *Pinus canariensis* forest in Tenerife, Canary Islands, An approach based on sap flow measurements. *Environmental Pollution* 140, 383-386.
- Wieser, G., Matyssek, R., Köstner, B. and Oberhuber, W., 2003. Quantifying ozone uptake at the canopy level of spruce, pine and larch trees at the alpine timberline, an approach based on sap flow measurement. *Environmental Pollution* 126, 5-8.
- Yang, J., Yu, Q. and Gong, P., 2008. Quantifying air pollution removal by green roofs in Chicago. *Atmospheric Environment* 42, 7266-7273.
- Yin, S. et al., 2011. Quantifying air pollution attenuation within urban parks, An experimental approach in Shanghai, China. *Environmental pollution* 159, 2155-2163.
- Zhang, X., Zhang, P., Zhang, Y., Li, X. and Qiu, H., 2007. The trend, seasonal cycle, and sources of tropospheric NO₂ over China during 1997–2006 based on satellite measurement. *Science in China Series D, Earth Sciences* 50, 1877-1884.

- Zhang, Y.H. et al., 2008. Regional ozone pollution and observation-based approach for analyzing ozone–precursor relationship during the PRIDE-PRD2004 campaign. *Atmospheric Environment* 42, 6203-6218.
- Zheng, J., Zhang, L., Che, W., Zheng, Z. and Yin, S., 2009. A highly resolved temporal and spatial air pollutant emission inventory for the Pearl River Delta region, China and its uncertainty assessment. *Atmospheric Environment* 43, 5112-5122.
- Zhu, L.W. et al., 2012. Effects of sap velocity on the daytime increase of stem CO₂ efflux from stems of *Schima superba* trees. *Trees* 26, 535-542.
- Zimmermann, F., Plessow, K., Queck, R., Bernhofer, C. and Matschullat, J., 2006. Atmospheric N-and S-fluxes to a spruce forest—Comparison of inferential modelling and the throughfall method. *Atmospheric Environment* 40, 4782-4796.